ROLLING BALL SCULPTURE AS A MECHANICAL DESIGN CHALLENGE

Alma Žiga[1], Derzija Begic-Hajdarevic[2]
[1](University of Zenica, Faculty of Mechanical Engineering,
aziga@mf.unze.ba)
[2](University of Sarajevo, Faculty of Mechanical Engineering,
begic@mef.unsa.ba)

ABSTRACT:
Rolling ball sculpture, even the simple one, can be viewed as mechanical design challenge. If sculpture is made of poplar plywood, then bending and twisting of track causes stresses which can destroy rails of track. Another aspect is kinematic and dynamics of rolling ball. Sections of track where the rails is closer together will cause the ball to roll faster, but the ball is more likely to fall off the track. Centripetal force acting on the ball on spiral path increases own intensity with square of velocity and might cause ball to fall off. All these aspects will be analyzed in the paper.
Keywords: rolling ball sculpture, stress analysis in plywood semicircle console, kinematic and dynamics of ball rolling on a track.

----

1. INTRODUCTION

A rolling ball sculpture (sometimes referred to as a marble run, ball run, gravitram, kugelbahn, or rolling ball machine) is a form of kinetic art. Even though a rolling ball sculpture can range from simple to extremely complex, it is always grounded to the simple movement; a ball rolling on a track. When ball is positioned at the top of the track, and is let to go, the gravity becomes the motive force. Utilization of creative track designs to harness the energy of the rolling ball leads to amazing things that can be achieved. The rolling ball can be used to captivate, demonstrate, and educate on many levels. From small single track sculptures, to room-filling complex installations, each sculpture works in harmony with both the environment and with the experiences of the viewers [1]. Adding the laser cut parts, gears, handle, slots for lifting the balls, the simple movement has been elevated to a work of mechanical art.

Idea for sculpture, described in this paper, was conceived during watching YouTube channel Build Amazing Big Marble Run Machine [2]. Design was obtained in CAD software SolidWorks (Fig. 1.). All parts of sculpture were made from poplar plywood, 4 mm thick. After design and analysis all parts were cut from plywood sheet by laser cutter (Fig. 2.). Dimensions of Front and Back plate are 280x290 mm. Plates are 16 mm set apart. Between them is big toothed wheel with slots for balls to drop in when rolled down the track. Big wheel meshes with three small gears, one of which has handle to set big wheel in motion and to lift balls to the beginning of the track. The track forms left-hand, helix spiral with two revolutions. Spiral track has central dimensions: radius 120 mm and height 160 mm. Cross section of rail is rectangle 8x4mm. Rails is spaced for 8 mm (Fig. 7c). Balls are made of steel and have diameters of 11.4 mm. For assembly, track was made of four, half-revolution spirals. As the two rails of the track should be bent and

twisted to obtain 40 mm deflection, stress analysis should be done for inner rail, with smaller diameter. Another design concern is distance between rails as it means ball stability and ratio of its translational to rotational velocity. And the last analysis is dynamic of ball rolling on track.
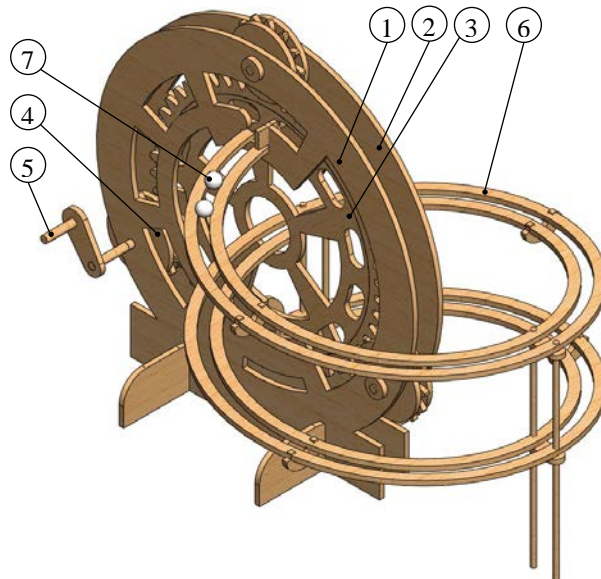
Fig. 1. SolidWorks design of rolling ball sculpture: 1-Front plate, 2-Back Plate, 3-Toothed wheel with slots, 4-Small gear, 5-Handle, 6-Track and 7-Ball

Fig. 2. Rolling ball sculpture

2. DEFLECTION OF INNER RAIL AS A HALF-CIRCLE CONSOLE

The deflection of the half-circle console end (at the point of application of the force P and in the direction of the force, Fig. 3) will be determined, as it is done in papers: [3], Horibe T. & Mori K. (2015), [4], Dahlberg T. (2004) and [5], Žiga A. et al. (2018). The force P is normal to the xy plane.
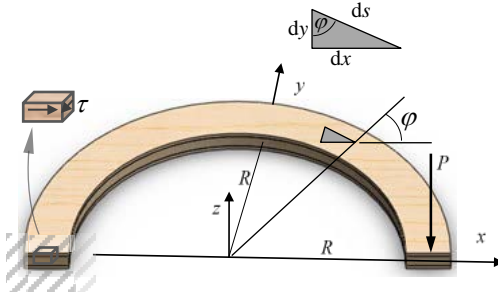
Fig. 3. Half-circle console   **Fig. 4.** Moments equilibrium
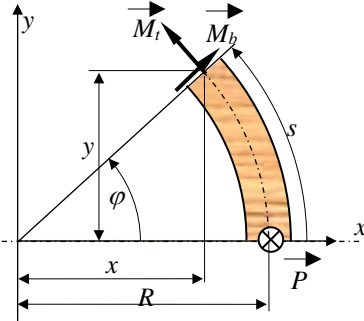
Fig. 4 shows cross-section of the beam situated at angle φ. The bending moment M_b and torsional moment M_t are acting at this cross-section. The shear force has been omitted in the figure, since its influence on beam deflection can be neglected. The equilibrium of moments is used, equations are obtained and solving for M_b and M_t gives:

$$M_b = -P\left[y\cos\varphi + (R-x)\sin\varphi \right]$$
$$M_t = P\left[(-R+x)\cos\varphi + y\sin\varphi \right] \tag{1}$$

Elastic strain energy stored in the beam is:

$$U = \frac{1}{2EI}\int_0^L M_b{}^2 \mathrm{d}s + \frac{1}{2GK_t}\int_0^L M_t{}^2 \mathrm{d}s \tag{2}$$

Where: L is the length of the half-circle console, E is modulus of elasticity, G is shear modulus, I is second moment of cross-sectional area, K_t is the cross-sectional factor of torsional rigidity.

Using Castigliano's theorem, the deflection of the console end, at the load P, can be calculated:

$$\delta = \frac{\partial U}{\partial P} = \frac{1}{2EI}\int_0^L 2M_b\frac{\partial M_b}{\partial P}\mathrm{d}s + \frac{1}{2GK_t}\int_0^L 2M_t\frac{\partial M_t}{\partial P}\mathrm{d}s \tag{3}$$

With M_b, M_t, $\partial M_b/\partial P$ and $\partial M_t/\partial P$ from (1), deflection is:

$$\delta = \frac{P}{EI}\int_0^L \left[-y\cos\varphi - (R-x)\sin\varphi \right]^2 \mathrm{d}s + \frac{P}{GK_t}\int_0^L \left[(-R+x)\cos\varphi + y\sin\varphi \right]^2 \mathrm{d}s \tag{4}$$

Expressions for $\sin\varphi, \cos\varphi, \mathrm{d}s, y, \mathrm{d}y/\mathrm{d}x$ can be obtained by geometry (Fig. 3.) and replaced in Equation (4). The integration over $\mathrm{d}s$ from 0 to L becomes integration over $\mathrm{d}x$

from R to -R. With substitution of dimensionless integration variable $t=x/R$, the integrals have limits 1 and -1.

$$\delta = \frac{PR^3}{EI}\int_{1}^{-1} -\sqrt{1-t^2}\,\mathrm{d}t + \frac{PR^3}{GK_t}\int_{1}^{-1}\frac{(-1+t)\sqrt{1-t^2}}{(1+t)}\,\mathrm{d}t \tag{5}$$

$$\delta = \frac{PR^3}{EI}1,5708 + \frac{PR^3}{GK_t}4,71239 \tag{6}$$

Deflection of half-circle console consists of two parts: due to bending and due to torsion. So in order to evaluate contribution of these parts to whole deflection, isotropic wooden material will be considered. Poplar veneer has three modulus of elasticity and three values of Poisson ratio. These values have been taken from the paper [6], Brezović, Mladen Vladimir, J. and Stjepan, P. (2003). One mean value is calculated for modulus of elasticity and Poisson ratio: $E = 3633$ MPa, $v = 0.35$. Shear modulus is calculated by the expression: $G=E / [2(1+v)]$ and has a value: $G = 1346$ MPa. Dimensions of half-circle, inner track are: radius-$R=112$ mm and cross-sectional dimensions (bxh) - 8x4 mm. Axial moment of inertia is $I_x = b \cdot h^3 / 12 = 8 \cdot 4^3 / 12 = 42.67$ mm^4.

The factor of torsional rigidity is $K_t = c_2 b \cdot h^3 = 0,229 \cdot 8 \cdot 4^3 = 117.25$ mm^4, where c_2 is coefficient for rectangular bar in torsion, taken from the book [7], Beer, F. P. (2014), Mechanics of Materials.

Solving equation (6) for unknown force, where, at the end of half-circle console, deflection is δ=40 mm, gives force value of P=0.7117 N. There, part of deflection due to bending is 10.1 mm and part of deflection due to torsion is 29.9 mm. So for isotropic wooden half-circle console, torsion has much more influence on deflection than bending.

Coordinates of the console clamp are: $\varphi = \pi$, $x = R\cos\varphi = -112$ mm, $y = R\sin\varphi = 0$.
Using equation (1), bending and torsional moments in the clamp are:
$$M_b = 0, \quad M_t = 159.42\,\mathrm{Nmm}.$$
Bending and torsional stresses in the clamp are:

$$\sigma_{bend} = \frac{6M_b}{bh^2} = 0 \quad \tau_{torsion} = \frac{M_t}{c_1 bh^2} = 5.063\,\mathrm{MPa} \tag{7}$$

Where coefficient c_1 depends only upon the ratio b and h. For $b/h = 8/4 = 2$, coefficient is: c_1=0,246.

With stress element $\sigma_x = 0$, $\sigma_y = \sigma_{bend} =0$ and $\tau_x = \tau_{torsion} = 5.063$ MPa, principal stresses are:

$$\sigma_{1,2} = \frac{\sigma_x + \sigma_y}{2} \pm \sqrt{\left(\frac{\sigma_x - \sigma_y}{2}\right)^2 + \tau_{xy}^2} = \pm 5.063\,\mathrm{MPa} \tag{8}$$

Ekvivalent, von Mises stress is:

$$\sigma_{vonMises} = \sqrt{\sigma_1^2 - \sigma_1\sigma_2 + \sigma_2^2} = 8.77\,\mathrm{MPa} \tag{9}$$

For numerical analysis of deflection, the inner rail was modeled and meshed (Fig. 5). The left side was clamped and at the right side, vertical translation of outer, lower vertex was set to be 40 mm. The study gave maximal, von Mises stress of the value 8.791 MPa, near the clamp (Fig. 6).
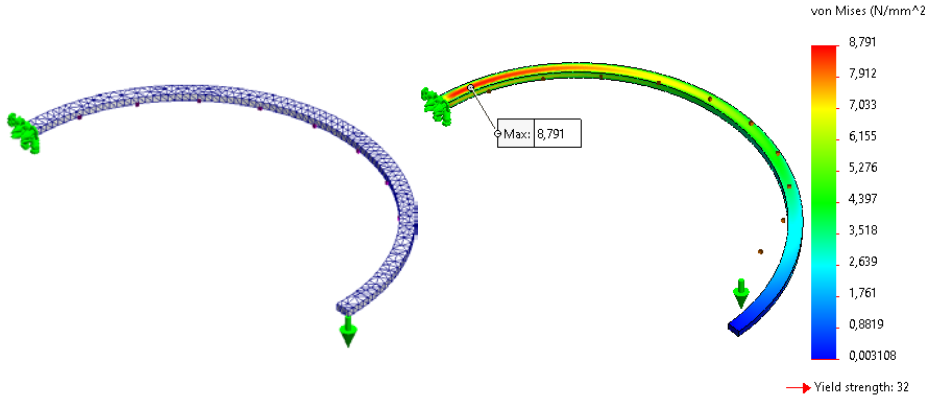
Fig. 5. Boundary conditions and meshing

Fig. 6. Von Mises stress in inner track due to deflection

3. TRACK RAILS SPACING AND BALL KINEMATICS

The spacing between the two rails of the track is an optimization between the security of the ball on the track and ball spin relative to its linear velocity.

Consider a ball rolling over a horizontal, frictional surface (Fig. 7a). Let v_C be the translational velocity of the ball's center of mass, and let ω be the angular velocity of the ball about an axis passing through its center of mass. Consider the point B of contact between the ball and the surface. The velocity v_B of this point is made up of two components: the translational velocity v_C, which is common to all elements of the ball, and the tangential velocity $v_t = \omega \cdot R$ due to the ball's rotational motion. Thus, $v_B = v_C - v_t = v_C - \omega \cdot R$. Suppose that the ball rolls without slipping. In other words, suppose that there is no frictional energy dissipation as the ball moves over the surface. This is only possible if there is zero net motion between the surface and the bottom of the ball, which implies $v_B = 0$ or $v_C = v_t$ or $v_C = \omega \cdot R$. The ratio of translational velocity to the tangential velocity of the bottom of the ball is: $v_C / v_t = 1$.

However, if the point that the ball is rolling on changes to two points, the ratio changes. A certain angle θ is subtended by the radius of ball contact point with the vertical (Fig. 7c). Let ω be the angular velocity of the ball. Let v_C be the translational velocity of the ball's center of mass: $v_C = \omega \cdot b$ (Fig. 7b), where b is the height of the center of mass from the axis connecting the points of contact. Consider the point B at the bottom of the ball. The velocity v_B of this point is made up of two components: the translational velocity v_C and the tangential velocity $v_t = \omega \cdot R$ due to the ball's rotational motion. Thus, $v_B = v_C - v_t = \omega \cdot b - \omega \cdot R$. The ratio of translational velocity to the tangential velocity of the bottom of the ball is: $v_C / v_t = b / R = \cos\theta$.

Sections of track where the rails were closer together would cause the ball to roll faster, at the cost of stability, as the ball was more likely to fall off the track. Increasing the distance between the rails would cause the ball to roll slower, but would increase the odds that the ball stayed on the track.
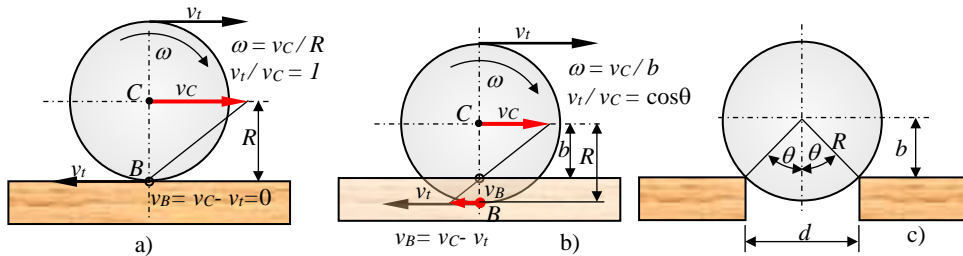
Fig. 7. A ball rolling over a rough surface: a) one point contact b) two point contact c) distance between rails.

For the given track, distance between rails is $d = 8$ mm. For radius of steel ball $R = 5.7$ mm, angle subtended by the radius of ball contact point with the vertical is $\theta = 44.56°$. The ratio of translational velocity to tangential velocity of bottom ball point is $v_C / v_t = b / R = \cos\theta = 0.71$. This angle yields a good balance between security on the track and translational velocity to tangential velocity ratio.

3. BALL DYNAMICS DURING ROLLING DOWN THE TRACK
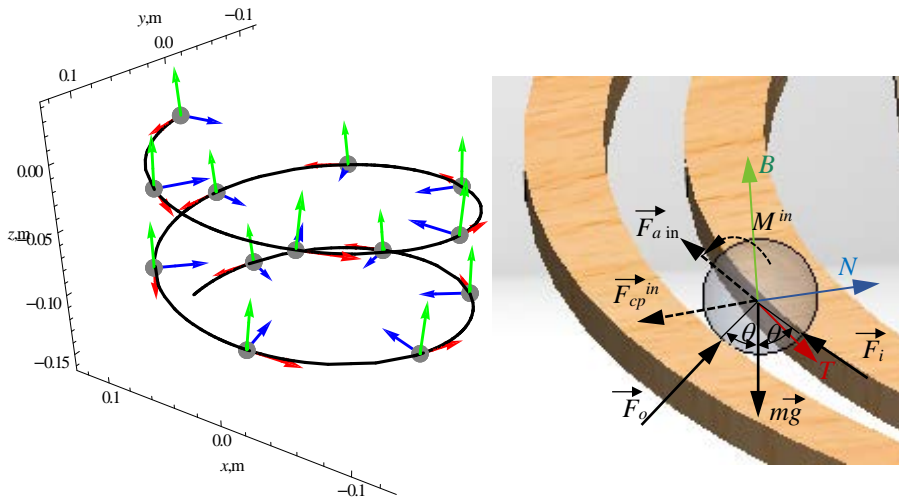
Fig. 8. A ball rolling down: a) natural coordinate system b) all forces and moments acting on the ball

Using d'Alembert's principle, rolling ball can be transformed into an equivalent static system by adding the so-called "inertial forces" and "inertial torques" or moments [8]. The ball can then be analyzed as a static system subjected to this "inertial forces and moments" and the external forces and reactions. Assuming that friction is negligible, forces that act on rolling ball are (Fig. 8b): inertial forces due to tangential and centripetal acceleration,

inertial moment due to angular acceleration, reaction forces due to contacts with inside and outside rail, and active force of gravity.

The local, normal and tangential (natural) coordinate system for certain points along the path are shown in Fig. 8a, using Mathematica software [9]. For given a parameterized path $r(s)$, definition of unit vectors in tangential, normal and binormal directions are:

$$\vec{u}_T = \frac{\vec{r}\,'(s)}{\left|\vec{r}\,'(s)\right|} \quad \vec{u}_N = \frac{\vec{u}_T\,'(s)}{\left|\vec{u}_T\,'(s)\right|} \quad \vec{u}_B = \frac{\vec{r}\,'(s) \times \vec{r}\,''(s)}{\left|\vec{r}\,'(s) \times \vec{r}\,''(s)\right|} \tag{10}$$

Path as a vector is $\vec{r}(s) = \left\{ 0.12\cos t, 0.12\sin t, -\dfrac{0.04}{\pi}t \right\}$, where t is in interval $\{t, 0, 4\pi\}$ for two revolutions spiral.

Static equilibrium conditions in normal and binormal coordinate system are:

$$\begin{aligned} \Sigma F_{N\,i} = 0 \quad & F_o \sin\theta - F_i \sin\theta + F_{cp}^{\ in} = 0 \\ \Sigma F_{B\,i} = 0 \quad & F_o \cos\theta + F_i \cos\theta + m\vec{g}.\vec{u}_B = 0 \end{aligned} \tag{11}$$

$F_{cp}^{\ in}$ is centripetal force, $F_{cp}^{\ in} = mv^2\nu$, where ν is a curve of the path: $\nu = \dfrac{\left|\vec{r}\,'(s) \times \vec{r}\,''(s)\right|}{\left|\vec{r}\,'(s)\right|^3}$.

Velocity of ball can be calculated using energy conservation. The system is closed, so energy must be conserved. Initially the ball is at rest, so at this instant it contains only potential energy. When it travels along the track, it has potential energy and kinetic energy (translational and rotational).

$$mgr_z(0) = mgr_z(s) + \frac{m \cdot v(s)^2}{2} + \frac{1}{2}I_c \cdot \omega(s)^2 \tag{12}$$

Where m is the mass of the object, I_c is the moment of inertia about ball's center of mass $I_c = \dfrac{1}{2}mR^2$, $r_z(s)$ is the height of the center of mass at position s and b is the height of the center of mass from the axis connecting the points of contact (Fig.7b).

Using the definition of angular velocity $\omega = \dfrac{v(s)}{b}$, we can relate it to $v(s)$. Then, above equation gives ball's center velocity:

$$v(s) = \sqrt{\frac{2mg\left[r_z(0) - r_z(s)\right]}{\left(m + \dfrac{I}{b^2}\right)}} \tag{13}$$

Fig. 9a shows ball velocity vector as ball rolls down. It can be seen its increase in intensity, due to conversion of potential energy. Fig. 10b shows values of velocity during two revolutions of spiral path. The velocity square is a function of the vertical coordinate for a given path point $r_z(s)$.
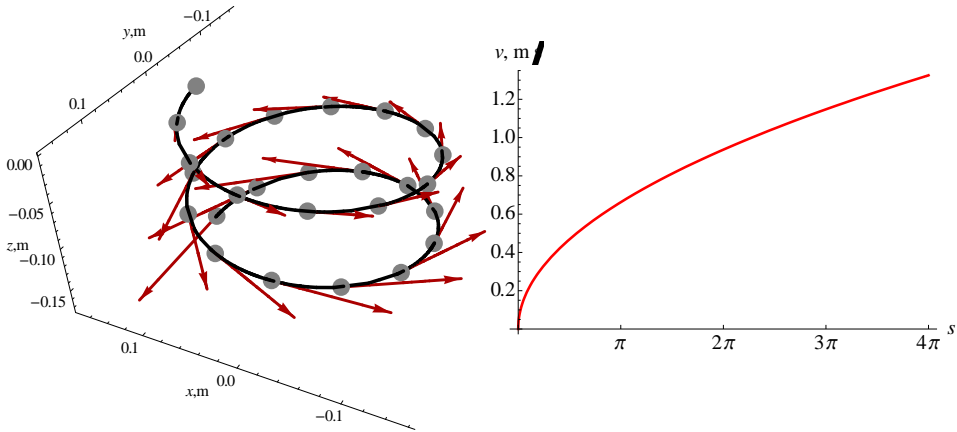
Fig. 9. Ball velocity a) vector drawn on path b) intensity

Solving equilibrium conditions in normal and binormal directions (eq.11) gives intensity of path reactions. These are: reaction on outside rail F_o and reaction on inside rail F_i. Reaction on outside rail increases due to increase of centripetal force. Opposite, reaction on inner rail decreases and near the end (3/4) of third half-revolution it becomes zero. Because of this all third part of path was needed to be fenced as was shown on Fig. 2.
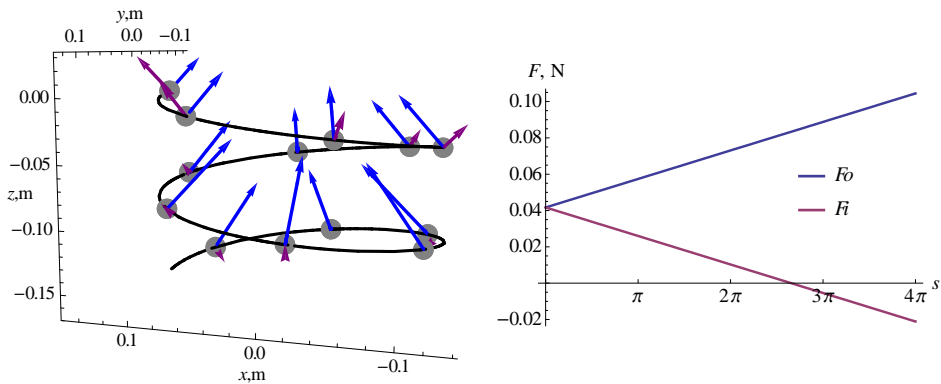
Fig. 10. Track reactions on outside and inside rail a) vectors drawn on path b) intensity

4. CONCLUSION

Rolling ball sculpture gives possibility to apply knowledge that is being acquired during Mechanical courses on technical faculty. Another aspect is artistic component of design. Every student can express its vision of sculpture. Sculpture can be conceived as an idea, modeled in SolidWorks, analyzed and then 'digitally' produced by laser cutter. Another interesting aspect toward finished product is an assemblage. No matter how design is detail and every aspect is analyzed, there are always some unpredicted circumstances that should

be overcome. In this structure, third part of spiral track needed to be fenced, because ball was jumping out of this part. Analysis was shown that in this part, inner reaction was become zero due to centripetal force, so ball was in contact only with outer rail of track.

4. REFERENCES

[1]   Boes, Eddie. "Rolling Ball Sculptures by Kinetic Artist Eddie Boes." Eddie's Mind, www.eddiesmind.com/.

[2]   Mini Gear, (2018, July 14). Build Amazing Big Marble Run Machine - DIY. YouTube. https://www.youtube.com/watch?v=LF0aDmlM5XU&feature=youtu.be

[3]   Horibe, T., Mori, K. (2015). In-plane and Out-of-plane Deflection of J-shaped Beam. Journal of Mechanical Engineering and Automation, 5(1), 14-19.

[4]   Dahlberg, T. (2004). Procedure to calculate deflections of curved beams. International journal of engineering education, 20(3), 503-513.

[5]   Žiga, A., Cogo, Z., Kačmarčik, J. (2018). Out-of-plane deflection of J-shaped beam. Proceedings of the 21th International Research/Expert Conference, TMT 2018. pp.269-272.

[6]   Brezović, M., Jambreković, V., Pervan, S. (2003). Bending properties of carbon fiber reinforced plywood. Wood research (Bratislava), 48(4), 13-24.

[7]   Beer, F. P., Johnston, R., Dewolf, J. & Mazurek, D. (2014). Mechanics of Materials, 7th Edition, McGraw-Hill.

[8]   Halliday, D., Resnick, R., & Walker, J. (2013). *Fundamentals of physics*. John Wiley & Sons.

[9]   Wolfram, S. (1999). *The MATHEMATICA® book, version 4*. Cambridge university press.

CORRESPONDANCE:

Alma Žiga, Ass. D.Sc. Eng.
University of Zenica
Faculty of Mechanical Engineering
St. Fakultetska 1
72000 Zenica, Bosnia and Herzegovina
E-mail: aziga@mf.unze.ba

Derzija Begic-Hajdarevic, Full professor
University of Sarajevo
Faculty of Mechanical Engineering
Vilsonovo setaliste 9
71000 Sarajevo, Bosnia and Herzegovina
e-mail: begic@mef.unsa.ba